RASĀYAN *J. Chem.*
Vol. 18 | No. 2 |1200-1206| April - June | 2025
ISSN: 0974-1496 | e-ISSN: 0976-0083 | CODEN: RJCABP
http://www.rasayanjournal.com
http://www.rasayanjournal.co.in

EFFICIENT BIFUNCTIONAL SYNTHESIS OF A SENSITIVE ELECTROCHEMICAL SENSOR FOR DETECTING ENDOCRINE DISRUPTING PLASTICIZERS

F. Janeeta Priya[1,✉], A. Leema Rose[1], S. Vidhya[1], A. Arputharaj[2] and A. Revathii[1]

[1]PG and Research Department of Chemistry, Holy Cross College (Affiliated to Bharathidasan University), Tiruchirappalli- 620002, Tamil Nadu, India

[2]Department of Electronics, St. Joseph's College (Affiliated by Bharathidasan University), Tiruchirappalli 620002, Tamil Nadu, India

✉Corresponding author: janeetapriya@hcctrichy.ac.in

ABSTRACT

A potential endocrine-disrupting chemical (EDC), Bisphenol A (BPA), has a detrimental effect on the health of humans and the environment. BPA is a plasticizer that is found in metal food packaging, plastic water vessels, and canned beverages. Consequently, it is imperative to create a BPA detection technology that is both highly sensitive and efficient, as well as practical. In this study, we present the facile synthesis of MoS_2 and MoS2-doped rGO nanoparticles, which are produced through a hydrothermal method, and their application in BPA sensing. A remarkable BPA detection instrument has been generated by the synthesized nanoparticles. Physicochemical methods, including XRD, SEM, EDAX, and FTIR, have been employed to examine the form and composition of MoS_2 and MoS_2-rGO nanoparticles. MoS_2 and MoS_2-rGO nanomaterials were employed to identify BPA using electrochemical methods, including Cyclic Voltammetry. A straightforward drop-casting procedure is employed to encapsulate both synthesized materials in GCE. This method has the potential to provide novel opportunities for the electrochemical detection of BPA in practical environments.

Keywords: Bisphenol A, MoS_2-rGO, Electrochemical Sensing, Cyclic Voltammetry, Glassy Carbon Electrode.

RASĀYAN *J. Chem.*, Vol. 18, No. 2, 2025

INTRODUCTION

Bisphenol A disrupts the endocrine system, significantly impacting human health and the environment. BPA is both a polymer and an epoxy chemical that is ubiquitous in our everyday lives and environments. BPA may contaminate nutrition, beverages, the environment, and sediment. It accumulates in many individual body regions and tissues, using distinct molecular pathways that may be detrimental to human health.[1-4] Consequently, it is imperative to create a practical, highly sensitive, and efficient BPA detection technique. A variety of analytical methods have been proposed for the measurement of BPA. While these technologies exhibit high sensitivity and reproducibility, they are costly, time-consuming, and require specialized personnel to operate the equipment. Electrochemical methods have emerged as effective options for detecting BPA, offering several advantages such as cost-effectiveness, high sensitivity, clarity, specificity, and portability.[4] MoS_2-rGO nanocomposites have recently garnered increased interest due to the comparability of MoS2 to graphene. MoS_2 is an inorganic compound classified within the transition metal dichalcogenides (TMDs) group, composed of a single molybdenum atom and two sulfur atoms. Three atomic layers (S-Mo-S) are arranged in a stacked configuration, held together by weak interactions that are enabled by van der Waals forces. MoS_2 has exceptional physical and chemical properties that have garnered significant attention from scientists for many applications, including lithium-ion batteries with rechargeable capabilities, solar panels, heterogeneous catalysts, supercapacitors, and sensors.

The distinctive properties of graphene, such as its rapid electron mobility, extensive surface area, and exceptional mechanical strength, make it a very attractive material. Reduced graphene oxide (rGO) has uses in anti-corrosion and lubrication. As a result, graphene is often used as an electrode in electrochemical applications, including supercapacitors, the oxygen reduction reaction (ORR)[5,6], biosensors, and electrochemical sensors. This project entails the creation of an electrochemical sensor aimed at identifying harmful endocrine-disrupting plasticizers through the utilization of MoS_2-doped reduced graphene oxide. The generation of MoS_2 composites on the surface of rGO is achieved through a straightforward hydrothermal method.

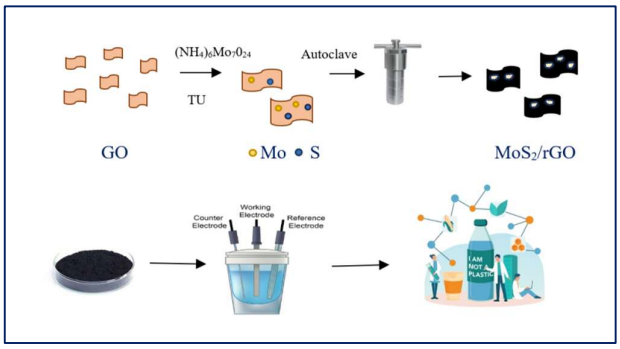

Fig.-1: Synthesis of MoS_2-rGO and its use as an Electrochemical Sensor

EXPERIMENTAL

Collection of Chemicals

Graphene oxide, thiourea, ammonium molybdate heptahydrate from Sigma-Aldrich, and BPA from Rankay Chemicals were used in this investigation.

Combination of Molybdenum Disulfide

MoS_2 was synthesized using the hydrothermal technique. 0.37 g of $(NH_4)_6Mo_7O_{24}$ and 0.638 g of (CH_4N_2S) were measured and thereafter transferred to a 50 ml container. The jar is thereafter filled with 30 milliliters of double-distilled water. The sample was maintained at room temperature using a magnetic stirrer for one hour. After the liquid was blended for one hour, it was put in a 50 ml autoclave. The sample underwent autoclaving in a hot-air oven for a duration of 24 hours at a temperature of 160 °C. Subsequent to autoclaving, the sample solution was allowed to cool to room temperature. The resulting solution was subjected to many centrifuge cleanings at about 2500 rpm using distilled water and ethanol. The gathered black residue was desiccated overnight at 60 °C in an oven.

Synthesis of Molybdenum Disulfide /Reduced Graphene Oxide

0.045 g of Graphene Oxide was measured, and a stable solution was prepared by dispersing the measured graphene oxide in 30 ml of double-distilled water and exposing it to sonication for one hour. After one hour, Ammonium molybdate heptahydrate ($(NH_4)6Mo_7O_{24}$) and Thiourea (CH_4N_2S) were weighed and added to the GO dispersed solution. The sample solution was maintained in a magnetic stirrer. The protocol for synthesizing MoS_2 is outlined herein. Throughout this procedure, Graphene oxide is reduced and transformed into Reduced Graphene oxide.

FT-IR Spectroscopy

FTIR serves as a method for identifying the functional groups that are present within the material. Wavenumber serves as a crucial metric in the FTIR spectrum, as it is intrinsically linked to energy and frequency, thereby enhancing the interpretation of the spectrum.[7-9]

SEM Analysis

Scanning Electron Microscopy is utilized to analyze the dimensions and morphology of the molecule[9]. SEM serves as a widely utilized method for the examination of nano-scale characteristics of graphene, including wrinkles, folding lines, and grain structures, especially in the context of CVD-grown graphene. Its non-contact nature, typically non-destructive approach, and relative ease of use make it an effective tool for rapid analysis when compared to alternative characterization techniques.[10-11]

Edax Analysis

EDAX serves as a technique for analyzing and detailing the chemical composition or elemental structure of a material. The ability to characterize is primarily due to the fundamental principle that each element possesses a unique atomic structure, leading to a specific set of peaks that form its electromagnetic emission spectra. This technique is fundamental to the field of materials science.

XRD Analysis

EDAX functions as a method for examining and specifying the chemical composition or elemental arrangement of a material. The capacity for characterization stems from the core principle that every element has a distinct atomic structure, resulting in a unique arrangement of peaks that constitute its electromagnetic emission spectra. This technique is essential to the discipline of materials science.[12]

Electrochemical Sensing of Bisphenol A

Instrumentation

The CH electrochemical analyzer serves the purpose of sensing materials and measuring supercapacitors. The system comprises three electrodes: a working electrode, a reference electrode, and a counter electrode. MoS_2 and MoS_2/rGO are utilized in GCE functioning as working electrodes. Platinum rod functions as the counter electrode, while Silver/Silver chloride operates similarly to the reference electrode. The three electrodes are submerged in a 0.20 M solution of the analyte BPA and Phosphate Buffer Sulphate. PBS serves as a supporting electrolyte solution in this context.

Fabrication of Electrode

The glassy carbon electrode's surface undergoes polishing through the application of alumina slurry. Subsequently, GCE underwent a cleaning process utilizing ethanol and double-distilled water, facilitated by sonication. The ink solution of MoS_2 was formulated by combining 2 mg of the dried sample (MoS_2) with 500 µL of ethanol. The prepared ink solution was applied to a glassy carbon electrode, which was then air-dried for several minutes before a second coating was applied. The procedure is executed three times. The identical procedure applies to the ink solution of MoS_2/Rgo.[13]

Electrochemical Measurement

Cyclic voltammetry was conducted at a scan rate of 50 mV, with a single cycle measured. The electrochemical activity was measured for a 50 µL sample of Bisphenol A, focusing on its electrolyte concentration. The electrochemical behavior of the synthesized MoS_2 and MoS_2/rGO in relation to the analyte material BPA was observed.

RESULTS AND DISCUSSIONS

Growth Mechanism

At the outset, one hour of ultrasonic treatment results in a well-distributed GO solution. Simultaneously, $(NH_4)_6Mo_7O_{24}$ and Thiourea (CH_4N_2S) were incorporated into the mixture that constituted the solution. The MoS_2/rGO pairs were synthesized using a hydrothermal method at a temperature of 160 ºC over a duration of 24 hours. The hydrophilic groups, identified as -OH or -COOH groups, present on each side of the GO during the hydrothermal response provide a robust foundation and framework for the incorporation of sulfur and molybdenum sources (Fig.-2). Furthermore, due to the functional characteristics of this group and the external defect of GO, graphene undergoes self-assembly through hydrothermal heating, facilitating the bonding of Mo atoms with C atoms.[14]

Fig.-2: Synthesize of the MoS_2 Doped rGO

FT-IR Spectroscopy

The functional group of the MoS2-doped Reduced Graphene Oxide was analyzed using FTIR Spectroscopy. Figure-3 illustrates the peak and stretching characteristics of the synthesized MoS2-doped rGO.

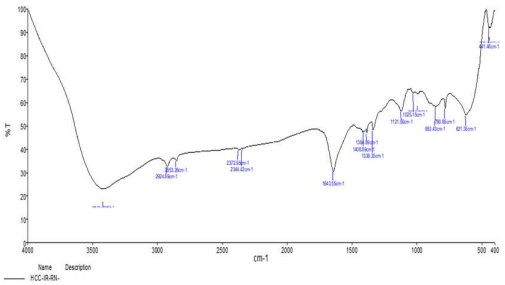

Fig.-3: FT-IR Peak and Stretching of the MoS_2 Doped rGO

The prominent and extensive peak at 3415.96 cm^{-1} indicates O-H Stretching, while the peak at 2924.89 cm^{-1} signifies the C-H Stretching of Alkanes. 1643.55 cm^{-1} demonstrate C=C Stretching of Alkenes observed at 1408.89 cm^{-1} C-C bending at 780.85 cm^{-1} is observed. The C-H bending (aromatic) and C-O stretching are indicated by the peak at 1025.15 cm^{-1}, while the peak at 990.03 cm^{-1} is also noted (Table-1). The presence of C=C bending in the functional group signifies the formation of rGO and plays a crucial role in confirming its existence within the nanohybrid structure.[15]

Table-1: Stretching and Peak of FT-IR Technique for MoS_2 Doped Rgo

S.No.	Functional group	Frequency (cm^{-1})
1	O-H Stretching	3415.96
2	C-H Stretching	2924.89
3	C=C Stretching	1643.55
4	C-C bending	1408.89
5	C-O Stretching	1025.15
6	C-H bending	780.85
7	C=C bending	990.03
8	Mo-S Stretching	441.46

SEM Analysis

MoS_2 nanoparticles have formed a hierarchical framework and are affixed to the rGO. GO is reduced to rGO via the hydrothermal method. The phenomenon of partial overlapping leads to the organization of rGO into a flexible architecture. The overlapping of the rGO forms a connected conducting network that facilitates rapid electron transfer, which is beneficial for sensor applications. The synthesized MoS2 nanoparticles measure approximately 80-90 nm in diameter and exhibit a spherical morphology is shown in Fig.-4.

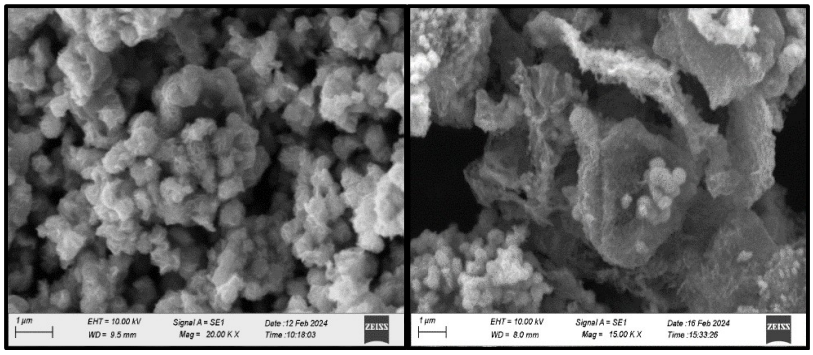

Fig.-4: SEM Analysis of Synthesized MoS_2 and MoS_2-rGO

Furthermore, the dispersion of MoS_2 nanoparticles on rGO can be attributed to the extensive surface area provided by graphene oxide. The synthesized MoS_2-doped rGO nanoparticles exhibit a size of approximately 90 nm and possess a spherical structure.[16]

EDAX

The EDAX analysis revealed the element's contour and the amount of synthesized MoS2-doped reduced graphene oxide present in the sample. The EDAX spectrum indicates that the sample components consist solely of Molybdenum, Sulfur, Oxygen, and Carbon.[17] The surfactant underwent a carbonizing process that resulted in the formation of the element C through the use of rGO (Fig.-5). The analysis indicates that the sample is free from impurities and exhibits a higher level of purity (Table-2).

Table-2: Synthesized MoS_2 Doped rGO Analysis from EDAX

S.No.	Element line	Weight %	Weight % error	Atom%
1	CK	47.43	7.98	70.25
2	OK	17.82	3.82	19.81
3	SK	9.45	0.31	5.24
4	MoL	25.30	0.77	4.69
5	Total	100		100

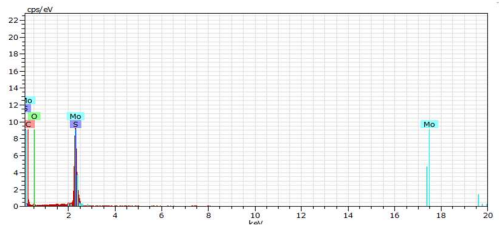

Fig.-5: EDAX Analysis of Synthesized MoS_2-rGO

XRD (X-RAY DIFFRACTION)

The crystallinenatureof the synthesized MoS_2 doped rGO is figure out by X-ray diffraction analysis. The synthesized MoS2-doped rGO is characterized through XRD analysis. Figure-6 illustrates the crystalline characteristics of the synthesized MoS2-doped rGO sample. The recorded peaks were at 13.690, 33.70, and 58.90, corresponding to the (002), (100), and (110) planes, respectively. 4 mg of Graphene oxide with MoS_2 exhibits d spacing measurements of 6.468 nm, 2.732 nm, and 1.566 nm (Table-3). The observed pattern reveals the absence of any supplementary crystal diffraction peaks, suggesting that the composite material consists solely of MoS_2 and rGO.[17-19]

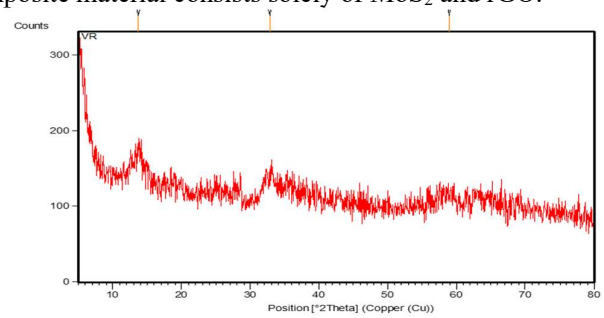

Fig.-6: XRD Diffraction Peak Values of Synthesized MoS_2 Doped rGO

Table-3: Synthesized MoS_2 Doped rGO Analysis from XRD

S. No.	Pos. [^{0}2 Th]	FWHM Left[^{0}2 Th]	d-spacing [A^0]	Height [cts]	Rel. Int [%]
1	13.6901	1.5744	6.46844	39.09	100.00
2	32.7739	1.5744	2.73262	27.51	70.36
3	32.7739	2.2042	1.56683	13.42	34.34

Cyclic Voltammetry

The sensing activity of GCE, MoS_2/GCE, and MoS2-doped reduced graphene oxide/GCE was recorded through cyclic voltammetry in a solution comprising 50 µl of BPA and 10 mL of PBS as the supporting electrolyte at pH 7.[20,21]

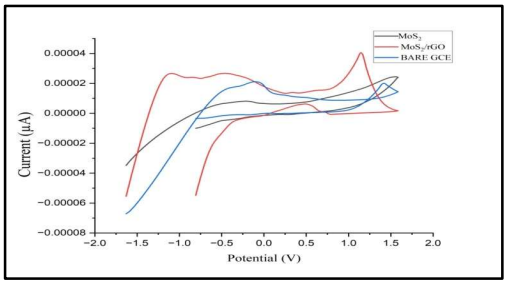

Fig.-7: CV of Bare GCE, MoS2, and MoS_2-rGO

The comparison plot of CV curves for GCE, MoS_2/GCE, and MoS_2-rGO/GCE reveals a lower electrochemical performance for GCE, while MoS_2/GCE demonstrates superior performance. The findings indicate that MoS_2-doped Reduced Graphene Oxide/GCE serves as an effective material for the detection of Bisphenol A. The comparison plot of bare GCE, MoS_2/GCE, and MoS_2/rGO/GCE indicates that MoS_2-doped reduced graphene oxide exhibits superior sensing activity when analyzing 50 µl of BPA (Fig.-7).

CONCLUSION

This endeavor involves the development of an electrochemical sensor that utilizes MoS2-doped rGO-bifunctional hybrids for the purpose of detecting the hazardous chemical Bisphenol A. MoS_2 and MoS2-

doped rGO were synthesized effectively using a hydrothermal method at 1600°C for a duration of 24 hours. The FT-IR spectra of the synthesized MoS2-doped rGO hybrids indicate the existence of multiple functional groups. The SEM analysis indicates that the produced MoS_2 and MoS2-doped rGO nanoparticles display a distinct spherical particle morphology. The crystallized state of the synthesized MoS_2-rGO is evaluated using X-ray diffraction analysis. EDAX analysis was performed to determine the elemental signals in MoS_2-rGO, focusing on the identification of Mo, C, S, and O. The electrochemical activity of the electrode was analyzed using 50 µL of BPA. The produced MoS_2-rGO demonstrated remarkable sensing performance with 50 µL of the analyte BPA. Future research aims to validate synthesized materials in actual samples containing BPA and to develop sensors for commercial applications that meet high-quality standards while remaining cost-effective.

ACKNOWLEDGMENTS

We would like to express our deepest regards to the Archbishop Casimir Instrumentation Center (ACIC), St. Joseph's College (Affiliated by Bharathidasan University), Tiruchirappalli 620002, Tamil Nadu, India, for their support and help toward characterization analysis.

CONFLICT OF INTERESTS

The authors declare that there is no conflict of interest.

AUTHOR CONTRIBUTIONS

All the authors contributed significantly to this manuscript, participated in reviewing/editing and approved the final draft for publication. The research profile of the authors can be verified from their ORCID ids, given below:

F. JaneetaPriya https://orcid.org/0000-0003-1872-8297
A. Leema Rose https://orcid.org/0000-0001-9978-2118
S. Vidhya https://orcid.org/0000-0001-7739-8035
A. Arputharaj https://orcid.org/0000000279815872
A.Revathi https://orcid.org/0009-0008-5739-3614

REFERENCES

1. B. S. Rubin, *The Journal of Steroid Biochemistry and Molecular Biology*, **127(1–2)**, 27(2011), https://doi.org/10.1016/j.jsbmb.2011.05.002
2. I. Cimmino, F. Fiory, G. Perruolo, C. Miele, F. Beguinot, P. Formisano and F. Oriente, *International Journal of Molecular Sciences*, **21(16)**, 5761(2020), https://doi.org/10.3390/ijms21165761
3. J. Kang, F. Kondo, and Y. Katayama, *Toxicology*, **226(2–3)**, 79(2006b), https://doi.org/10.1016/j.tox.2006.06.009
4. J. Kang, F. Kondo and Y. Katayama, *Toxicology*, **226(2–3)**, 79(2006), https://doi.org/10.1016/j.tox.2006.06.009
5. J. Sochor, J. Dobes, O. Krystofova, B. Ruttkay-Nedecky, P. Babula, M. Pohanka, T. Jurikova, O. Zitka, V. Adam, B. Klejdus and R.Kizek, *International Journal of Electrochemical Science*, **8(6)**, 8464(2013), https://doi.org/10.1016/s1452-3981(23)12902-6
6. D. Escalera-López, R. Griffin, M. Isaacs, K. Wilson, R. E. Palmer, and N. V. Rees, *Applied Materials Today*, **11**, 70(2018), https://doi.org/10.1016/j.apmt.2018.01.006
7. B. Singh, B. Prasad, and D. Kumar, *Semiconductors*, **55(1)**, 100(2021), https://doi.org/10.1134/s1063782621010152
8. S. A. Khan, S. B. Khan, L. U. Khan, A. Farooq, K. Akhtar, and A. M. Asiri, In *Springer eBooks* 317(2018), https://doi.org/10.1007/978-3-319-92955-2_9
9. Front Matter, *Elsevier eBooks*, iii(2017), https://doi.org/10.1016/b978-0-323-46140-5.01001-3
10. K. Vernon-Parry, *III-Vs Review*, **13(4)**, 40(2000), https://doi.org/10.1016/s0961-1290(00)80006-x
11. J. T. Quiñones, M. Yun, *Microelectronic Engineering*, **269**, 111915(2022), https://doi.org/10.1016/j.mee.2022.111915
12. V. Shanmugapriya, S. Arunpandiyan, G. Hariharan, A. Arivarasan, In *Materials Horizons,* pp. 533–567(2023), https://doi.org/10.1007/978-981-99-3021-0_22

13. M. A. Mutalib, M. Rahman, M. Othman, A. Ismail, J. Jaafar, In *Elsevier eBooks,* pp.161–179(2017), https://doi.org/10.1016/b978-0-444-63776-5.00009-7
14. J. Chen, Y. Xia, J. Yang, B. Chen, *Applied Physics A*, **124(6)**, Article 430(2018), https://doi.org/10.1007/s00339-018-1843-7
15. S. Li, Y. Chen, W. Liang, Y. Shao, K. Liu, Z. Nikolov, Y. Zhu, *Joule*, **2(9)**, 1838(2018), https://doi.org/10.1016/j.joule.2018.06.008
16. L. Zou, R. Qu, H. Gao, X. Guan, X. Qi, C. Liu, Z. Zhang, X. Lei, *Results in Physics*, **14**, 102458(2019), https://doi.org/10.1016/j.rinp.2019.102458
17. M. Gharani, A. Bahari, S. Ghasemi, *Journal of Materials Science Materials in Electronics*, **32(6)**, 7765(2021), https://doi.org/10.1007/s10854-021-05496-3
18. Y. Jiang, J. Ran, K. Mao, X. Yang, L. Zhong, C. Yang, X. Feng, H. Zhang, *Ecotoxicology and Environmental Safety*, **236**, 113464(2022), https://doi.org/10.1016/j.ecoenv.2022.113464
19. R. Singh, S. Agrohiya, S. Dahiya, I. Rawal, A. Ohlan, R. Punia, A. Maan, *Journal of Physics Conference Series*, **2663(1)**, 012022(2023), https://doi.org/10.1088/1742-6596/2663/1/012022
20. N. B. Messaoud, M. E. Ghica, C. Dridi, M. B. Ali, C. M. Brett, A. *Sensors and Actuators B Chemical*, **253**, 513(2017), https://doi.org/10.1016/j.snb.2017.06.160
21. S. Su, Q. Hao, Z. Yan, R. Dong, R. Yang, D. Zhu, J. Chao, Y. Zhou, L. Wang, *MicrochimicaActa*, **186(9)**, Article 607(2019), https://doi.org/10.1007/s00604-019-3678-0

[RJC-9227/2024]